

Robust control for aircraft anti-skid braking system based on dynamic tire/road friction force model

Li Fengyu

School of Automation Science and Electrical Engineering
Beijing University of Aeronautics and Astronautics
Beijing, China
alexander.lee1983@gmail.com

Jiao Zongxia

School of Automation Science and Electrical Engineering
Beijing University of Aeronautics and Astronautics
Beijing, China
zxjiao@buaa.edu.cn

Abstract—The aircraft anti-skid braking system plays an important role for the safety during taxiing. Aircraft tire/road friction force is essential information for model based control law. In this paper, a robust control strategy with an observer-based dynamic aircraft tire/road model is given to improve the brake quality. Firstly, the nonlinear fuselage and wheel models are derived. The tire/road friction force is derived with LuGre dynamic friction model considering velocity correlation, in which the internal friction state is estimated by dual-observer. In case of external disturbance and modeling error, a robust controller is employed to track the online calculated desired slip rate. The simulation results show that the well-designed controller has stable brake performance.

Keywords—aircraft braking control; LuGre dynamic friction model; robust control; state estimation; nonlinear control

I. INTRODUCTION

The reliability of the aircraft anti-skid braking system plays an important role for the safety of passengers and airports, which can stop the aircraft smoothly and effectively. When applying pressure on aircraft anti-skid braking system (ABS) during taking off, landing and taxiing, high efficiency control strategy is needed to ensure the aircraft ground safety. The aircraft braking system is a complex nonlinear system with uncertainties. The nonlinearities of system are constructed by the nonlinear relationship between aircraft tire and runway (or road) adhesion coefficient, adhesion coefficient and slip rate, and brake torque and pressure^[1]. It is rather difficult to get an accurate braking system and tire/road friction models and their parameters. Thus, nonlinear control theory is introduced to solve the problem mentioned above.

In the past, many kinds of control strategies were utilized in simulations, hardware-in-the-loop (HIL) experiments and aircraft tests. Most of the former research was not model based. The pressure bias control law is studied by Tang in [2], which shows reliable performance in simulation and tests. And the variable structure control and slip rate optimal control were also designed in the literatures^[3,4].

The tire/road adhesion force model is essential for model based control laws. Early research^[5] focused on the adhesion force representation, which is well-known as “Magic Formula”, gives a nice approximation to experimental results of the relationship between friction

coefficient and longitudinal slip. Recent research brings one kind of dynamic tire/road friction force model into ABS control, which has a potential advantage to describe closely some of the physical phenomena and to depend on parameters directly related with phenomena, called the LuGre Model. This model concerns the many-to-one mapping from velocity and other variables to adhesion coefficient^[6].

Many ABS control strategies are realized using the LuGre dynamic friction model under various road conditions. Especially, the parametric uncertainties due to road condition or/and temperature changing was considered in [7], in which one state observer was constructed to estimate internal friction state and longitudinal velocity. By utilizing LuGre dynamic friction force model, the desired maximum slip rate is estimated online. Thus, an observer-based braking controller is designed to track the desired slip rate. These models have been used successfully to identify and compensate the friction in mechanical system. In [8], a dual-observer was derived to capture different nonlinearities of friction state introduced by LuGre dynamic model, which can be used to improve the desired slip rate tracking performance. In case of possibility of entering non-robustness, an adaptive robust controller is designed to guarantee the stability of estimation^[9,10]. However, these strategies are developed without robust consideration.

In this study, the robust analysis is introduced to ABS control system. Firstly, the nonlinear fuselage and wheel models are established. The tire/road friction force is modeled by LuGre dynamic friction model considering velocity correlation, in which the unmeasurable internal friction state is estimated by dual-observer. The control target, desired slip rate, is calculated online with the help of pseudo-static distributed LuGre model. At last a robust controller for aircraft ABS is designed considering external disturbance like vertical load changing and modeling error. Simulations are implemented to verify the theoretical design.

II. SYSTEM DYNAMICS

A. Aircraft fuselage and wheel dynamics modeling

The aircraft ground dynamics model is shown in figure 1, from which we can see there are lift (L), engine thrust (T), aerodynamic drag (D), gravity (G) and landing gear forces acting on the fuselage. The landing gear forces are transferred from interaction between aircraft wheels and

runny, including longitudinal and normal nose landing gear force (F_{ln} and F_{nn}) and left and right main landing gear forces (F_{ll} , F_{lr} , F_{nl} and F_{nr}). When only considering the longitudinal forces, we have

$$m\dot{v} = T - D - F_{ln} - F_{lr} - F_{ll} \quad (1)$$

where v is aircraft longitudinal speed.

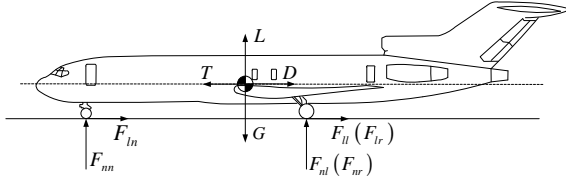


Figure 1 Forces on the fuselage

For the sake of simple, there are some assumptions below:

Assumption 1:

1) There are symmetric brake pressure signals between left and right braking system and same working conditions (runway state and temperature, etc.), thus, we have

$$F_x \triangleq F_{ll} = F_{lr} ; \quad (2)$$

2) There are no lateral forces or acceleration, which means that the vertical load has uniform distribution, thus, we have the same normal force

$$F_n \triangleq F_{nl} = F_{nr} ; \quad (3)$$

3) The fuselage gravity center speed v and aircraft wheel speed ω can be detected with sensors;

4) Longitudinal nose landing gear force (F_{ln}), engine thrust and lift are neglected account for their small magnitude compared with main landing gear longitudinal force (F_x) and gravity.

Remark 1: It is obviously that the system is ideally modeled and some conditions are ignored, which means that there must be model mismatch due to external disturbance and modeling error. And this term is defined as Δ_a which will be taken into consider later in the design of robust control.

Thus, based on **Assumptions 1**, we have

$$m\dot{v} = -2F_x - K_a v^2 . \quad (4)$$

where K_a is the aerodynamic drag coefficient and $D = K_a v^2$.

The aircraft wheel dynamics model is shown in figure 2, from which we can see the brake torque (u_τ) is applied on the rolling wheel. The brake torque magnitude has a complicated nonlinear relationship with brake valve order signal (P_b). But here we simplify it into linear relationship due to its high frequency response and weak effect on the control performance. The representation is $u = K_b P_b$, and $K_b = n_p \mu_p n_h A_p R_b$, which consists the informations of the friction faces of friction parts number (n_p), friction coefficient of friction parts (μ_p), brake piston number (n_h), piston area (A_p) and friction radius (R_b).

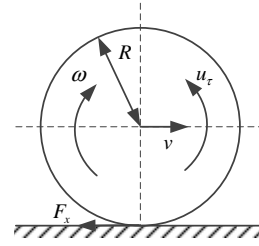


Figure 2 Dynamics of aircraft wheel

Thus, the aircraft tire model drafted in figure 2 can be described by

$$J\dot{\omega} = rF_x - K_b P_b \quad (5)$$

where J is rotational inertia of aircraft wheel and r is the wheel rolling radius.

B. Aircraft tire/road friction model

The aircraft tire/road friction coefficient is defined by the ratio of braking force and the normal force, which can be expressed as:

$$\mu = \frac{F_x}{F_n} , \quad (6)$$

where the friction coefficient μ is a complex function of the aircraft longitudinal slip and other factors, such as tire and runway conditions. The longitudinal slip is defined by:

$$\lambda = \frac{v - r\omega}{v} . \quad (7)$$

The dynamic tire/road contact friction model is described by the functions below [6]:

$$\frac{dz}{dt} = v_r - \frac{\sigma_0 |v_r|}{g(v_r)} z , \quad (8)$$

$$f_x(t) = (\sigma_0 z + \sigma_1 \frac{dz}{dt} + \sigma_2 v_r) F_n , \quad (9)$$

with

$$g(v_r) = \mu_c + (\mu_s - \mu_c) e^{-|v_r/v_s|^{1/2}}$$

where, z the internal weighted mean friction state, $v_r = (v - r\omega)$ is the relative velocity, f_x is the tire/road friction force model; σ_0 is the normalized rubber longitudinal lumped stiffness, σ_1 is the normalized rubber longitudinal lumped damping, σ_2 is the normalized viscous relative damping, μ_c is the normalized Coulomb friction, μ_s is the normalized static friction ($\mu_c \leq \mu_s, \in [0, 1]$), v_s is the Stribeck relative velocity.

Remark 2: z represents the wheel bristle deflection which an essential state variable for the friction force model [6]. And the value of z is unknown and unmeasurable, so observers are employed to estimate the magnitude of z , which will be studied in part III.

It is shown in [6] that the model has following finite bristle deflection property:

P1. If $|z(0)| \leq \mu_s / \sigma_0$, then $|z(t)| \leq \mu_s / \sigma_0, \forall t \geq 0$,

P2. $\infty > \mu_s \geq g(v_r) \geq \mu_c > 0, \forall v_r$.

Remark 3: **P1** is physically intuitive and used in the subsequent controller design for a guaranteed robust performance. And it ensures that the internal friction states are bounded and that its upper bound is given by the static friction parameter and bristle stiffness.

Considering the modeling error of entire system and LuGre model compared with the actual tire/road friction force

$$\Delta_m = F_x - f_x + \Delta_a, \quad (10)$$

where Δ_a is the system modeling error defined in **Remark 1**.

From (4) and (5), the whole system can be rewritten as:

$$m\dot{v} = -2f_x - K_a v^2 + 2\Delta_m, \quad (11)$$

$$J\dot{\omega} = f_x r - u_\tau + \Delta_m r. \quad (12)$$

III. ROBUST CONTROLLER DESIGN

A. Control target

The control law designed in this paper is in the purpose of making full use of the aircraft tire/road adhesion force/coefficient, which can shorten the braking distance. In the other words, a maximum deceleration is achieved with the same target. The desired slip rate λ_d is corresponding to the maximum adhesion force $F_{x\max}$ and coefficient μ_{\max} and v_{rd} is the desired relative speed corresponding to λ_d through the definition in (7). Thus, we can get the definition of braking efficiency by

$$\eta = \frac{\int_{\lambda_L}^{\lambda_H} \mu(\lambda)}{\mu_{\max}(\lambda_H - \lambda_L)}, \quad (13)$$

where, λ_H and λ_L are slip rate represent the first slip occurrence value and last brake releasing occurrence value. According to (13), it is known that high braking efficiency can be obtained by holding braking system working in the area around λ_d . By solving the distributed LuGre tire/road friction model and obtain the following pseudo-static relationship between μ and λ , we have

$$\mu = g(v_r) \left[1 + 2\gamma \frac{g(v_r)}{\sigma_0 L |\eta|} \left(e^{\frac{\sigma_0 L |\eta|}{2g(v_r)}} - 1 \right) \right] + \sigma_2 v_r, \quad (14)$$

with

$$\eta = \frac{\lambda}{1-\lambda}, \quad \gamma = 1 - \frac{\sigma_1 |\eta|}{r\omega g(v_r)},$$

where L is length of the tire/road contact patch.

Thus, assuming the parameters in equivalent pseudo-static model Equation (14) are known, the maximum slip rate λ_d corresponding to μ_{\max} can be calculated by solving it numerically. Then, v_{rd} is obtained for its definition. Thus, we have

$$\frac{dv_r}{dt} = \frac{dv}{dt} - r \frac{d\omega}{dt}. \quad (15)$$

Through linearly parameterizing the system model by substituting Equations (8), (9), (11), (12) to (15) gives

$$g_1 \frac{dv_r}{dt} = P_b - g_2 \sigma_0 z + g_2 \sigma_1 \frac{\sigma_0 |v_r|}{g(v_r)} z - g_2 (\sigma_1 + \sigma_2) v_r - \frac{g_1 K_a}{m} v^2 + \Delta$$

where, $g_1 = J/(rK_b)$, $g_2 = F_n(2J/m+r^2)/(rK_b)$, $\Delta = \Delta_m(2J/m+r^2)/(rK_b) + \Delta_n$.

Noting that, g_1 and g_2 are positive; Δ_n is the uncertain nonlinearity, so Δ represents the modeling error and uncertain nonlinearity.

Assumption 2: The modeling error and uncertain nonlinearity are bounded by a known positive constant

$$|\Delta| \leq \delta, \quad (16)$$

where δ is the known bound of Δ .

Obviously, the physical tire/road friction can serve limited adhesion force for the system, which can be treated as the maximum upper bound for δ .

B. Observers design

Based on the aircraft tire/road friction force description in (8) and (9), we can get the system dynamics represented by (11) and (12). Considering the description of part A in this section, the control target is to track the desired relevant speed v_{rd} obtained online by the calculation of desired slip rate λ_d . Thus, the entire system dynamics can be expressed in (16). Due to the unmeasurable internal friction state z , the observer should be employed to obtain it. Considering the different nonlinear characteristics of friction state z in the two terms $g_2 \sigma_0 z$ and $g_2 \sigma_1 \sigma_0 |v_r| z / g(v_r)$ of (16), a dual-observer structure is employed here which is proposed by Tan et al in [8]. This manipulation takes more flexibility to deal with different nonlinearities in the dynamics.

Theorem 1: In the case of the absence of uncertain nonlinearities and modeling error, i.e., $\Delta = 0$, suppose that the aircraft tire/road friction force is described by the model in (8) and (9), and consider the aircraft braking system equation in (11) and (12), the globally asymptotic tracking of online calculated desired slip rate λ_r , which is corresponding to μ_{\max} trajectory, is achieved by the following nonlinear control law:

$$P_{bn} = -k_1 e + g_2 \sigma_0 \hat{z}_0 - g_2 \sigma_1 \frac{\sigma_0 |v_r|}{g(v_r)} \hat{z}_1 + g_2 (\sigma_1 + \sigma_2) v_r + g_1 \dot{v}_{rd} + \frac{g_1 K_a}{m} v^2$$

where e represents the desired relative velocity tracking error and \hat{z}_0 and \hat{z}_1 represent the estimates of friction state.

The estimates of internal friction state z are obtained by the observers below to handle the different nonlinearities:

$$\frac{d\hat{z}_0}{dt} = v_r - \frac{\sigma_0 |v_r|}{g(v_r)} \hat{z}_0 - \gamma_0 e, \quad (18)$$

$$\frac{d\hat{z}_1}{dt} = v_r - \frac{\sigma_0 |v_r|}{g(v_r)} \hat{z}_1 + \gamma_1 \sigma_0 \frac{|v_r|}{g(v_r)} e, \quad (19)$$

where γ_0 and γ_1 are positive constants to be designed.

Proof: Base on the feedback linearization principles. With the choice of P_{bn} in (17), we have

$$g_1 \frac{de}{dt} = -k_1 e - g_2 \sigma_0 \tilde{z}_0 + g_2 \sigma_1 \frac{\sigma_0 |v_r|}{g(v_r)} \tilde{z}_1, \quad (20)$$

where the modeling error and uncertain nonlinearity $\Delta = 0$.

Define the following positive-semi-definite (p.s.d.) candidate Lyapunov function

$$V_n = \frac{1}{2} g_1 e^2 + \frac{1}{2\gamma_0} g_2 \sigma_0 \tilde{z}_0^2 + \frac{1}{2\gamma_1} g_2 \sigma_1 \tilde{z}_1^2. \quad (21)$$

It is worth announcing that, the observation errors in (21) can be described by (this will be utilized in the later proof)

$$\frac{d\tilde{z}_0}{dt} = -\frac{\sigma_0 |v_r|}{g(v_r)} \tilde{z}_0 + \gamma_0 e, \quad (22)$$

$$\frac{d\tilde{z}_1}{dt} = -\frac{\sigma_0 |v_r|}{g(v_r)} \tilde{z}_1 - \gamma_1 \sigma_0 \frac{|v_r|}{g(v_r)} e, \quad (23)$$

where $\tilde{z}_0 = z - \hat{z}_0$, $\tilde{z}_1 = z - \hat{z}_1$ and z is the unmeasurable real value of friction state.

The derivative of V_n along trajectories in (18), (19) and (20) is

$$\dot{V}_n = -k_1 e^2 - \frac{g_2 \sigma_0^2 |v_r|}{\gamma_0 g(v_r)} \tilde{z}_0^2 - \frac{g_2 \sigma_1}{\gamma_1} \frac{\sigma_0 |v_r|}{g(v_r)} \tilde{z}_1^2 \leq 0, \quad (24)$$

With P1, the real value (z), estimation value (\square_0, \square_1) and estimation errors (\tilde{z}_0, \tilde{z}_1) of friction state are bounded.

Based on the definition of v_{rd} , physical limitation of v and v_r , the boundedness of tracking error e is obvious. Due to the representations of g_2 and $g(v_r)$, the constants σ_0, σ_1 and σ_2 , the boundedness of controller is apparent from the structure in (17).

The boundedness of all internal variables and constants are proved. Thus, the derivative of the relative velocity tracking error e is also bounded. By (24), we have $e \in L_2$. Combining the fact that $e \in L_\infty$ and $\dot{e} \in L_\infty$ and utilizing the Barbalat's lemma, we conclude that, $e \rightarrow 0$, as $t \rightarrow \infty$. Thus, by the definition of e and λ in (7), we have $\lambda \rightarrow \lambda_d$, as $t \rightarrow \infty$.

C. Robust controller design

To avoid entering the unstable estimation of the unmeasurable friction states z , the following robust observers with projection-type modifications which are based on the observers design in part B

$$\frac{d\hat{z}_0}{dt} = Proj_{z_0} \left(v_r - \frac{\sigma_0 |v_r|}{g(v_r)} \hat{z}_0 - \gamma_0 e \right), \quad (25)$$

$$\frac{d\hat{z}_1}{dt} = Proj_{z_1} \left(v_r - \frac{\sigma_0 |v_r|}{g(v_r)} \hat{z}_1 + \gamma_1 \sigma_0 \frac{|v_r|}{g(v_r)} e \right). \quad (26)$$

The projection mapping $Proj_{z_i}(\cdot)$ has similar structure with Sastry in [11],

$$Proj_{z_i}(\cdot) = \begin{cases} 0 & \text{if } \zeta = \zeta_{max} \text{ and } * > 0 \\ 0 & \text{if } \zeta = \zeta_{min} \text{ and } * < 0 \\ * & \text{otherwise} \end{cases}, \quad (27)$$

where ζ is a symbol that can be replaced by z_0 and z_1 .

P2. The projection mapping has the following properties:

$$\tilde{z}_0 \left\{ Proj_{z_0} \left(v_r - \frac{\sigma_0 |v_r|}{g(v_r)} \hat{z}_0 - \gamma_0 e \right) - \left(v_r - \frac{\sigma_0 |v_r|}{g(v_r)} \hat{z}_0 - \gamma_0 e \right) \right\} \geq 0, \quad (28)$$

$$\tilde{z}_1 \left\{ Proj_{z_1} \left(v_r - \frac{\sigma_0 |v_r|}{g(v_r)} \hat{z}_1 + \gamma_1 \sigma_0 \frac{|v_r|}{g(v_r)} e \right) - \left(v_r - \frac{\sigma_0 |v_r|}{g(v_r)} \hat{z}_1 + \gamma_1 \sigma_0 \frac{|v_r|}{g(v_r)} e \right) \right\} \geq 0. \quad (29)$$

Lemma 1: Considering the aircraft braking system described in (11), (12) and tire/road friction force in the form of (8) and (9) with uncertain nonlinearities, i.e., $\Delta \neq 0$, we can find the nonlinear robust control law in the following structure

$$P_b = P_{bn} + P_{br}, \quad (30)$$

where P_{bn} is shown in (17). There exists a nonlinear robust control term P_{br} , in a form which satisfies the following relationships:

$$s = e \left(P_{br} - g_2 \sigma_0 \tilde{z}_0 + g_2 \sigma_1 \frac{\sigma_0 |v_r|}{g(v_r)} \tilde{z}_1 + \Delta \right) \leq \varepsilon, \quad (31)$$

where P_{br} is synthesized to attenuate the effect of the uncertain nonlinearities and modeling error, and ε is a constant to be designed. And

$$e P_{br} \leq 0. \quad (32)$$

Proof: Based on last part of the proof for Theorem 1, the internal friction state and parameters have the properties of boundedness. Thus, the robust control term P_{br} here always exists. Using the similar technique in Yao^[10], we choose smooth bounding function h satisfying:

$$h \geq g_2^2 \sigma_0^2 z_r^2 \left(1 + \sigma_1^2 \frac{|v_r|^2}{g^2(v_r)} \right) + \delta^2, \quad (33)$$

where $z_r = |z_{\max} - z_{\min}|$ (also exists $z_r = |\square_{0/1\max} - \square_{0/1\min}|$ by projection mapping in (25) and (26)).

And we choose the robust control term P_{br} in a form as

$$P_{br} = \frac{3}{4\varepsilon} h. \quad (34)$$

Thus, it is easily to have from (31) that

$$s \leq |e| P_{br} + |e| g_2 \sigma_0 z_r + |e| g_2 \sigma_1 \frac{\sigma_0 |v_r|}{g(v_r)} z_r + |e| \delta. \quad (35)$$

Substituting P_{br} into (35), we have

$$s \leq - \left(\frac{\sqrt{3} g_2 \sigma_0 z_r}{2\sqrt{\varepsilon}} |e| - \sqrt{\frac{\varepsilon}{3}} \right)^2 - \left(\frac{\sqrt{3} g_2 \sigma_1 \sigma_0 z_r |v_r|}{2\sqrt{\varepsilon} g(v_r)} |e| - \sqrt{\frac{\varepsilon}{3}} \right)^2 - \left(\frac{\sqrt{3} \delta}{2\sqrt{\varepsilon}} |e| - \sqrt{\frac{\varepsilon}{3}} \right)^2 + \varepsilon \leq \varepsilon \quad (36)$$

Thus the inequation in (31) is proved. According to the definition of e and P_{br} , it is easily to have that (32) is satisfied.

Theorem 2: Considering the aircraft braking system described in (11), (12) and tire/road friction force in the form of (8) and (9) with uncertain nonlinearities, i.e., $\Delta \neq 0$, we can find the nonlinear robust control law in the same structure as in (30), which is rewritten here as following,

$$P_b = P_{bn} + P_{br},$$

where P_{bn} is given in (17), the aircraft tire/road internal friction state observers are given in (25) and (26); P_{br} represents the robust control term in the form of (34), we have,

- 1) All the signals present in system are bounded. Furthermore, the candidate Lyapunov function in (39) satisfies:

$$V_r(t) \leq e^{-\frac{2k_1 t}{s_1}} V_r(0) + \frac{\varepsilon g_1}{2k_1} (1 - e^{-\frac{2k_1 t}{s_1}}), \quad (37)$$

- 2) If after a finite time t_0 , in absence of any uncertainties, i.e., $\Delta = 0$, by utilizing the proposed controller in (30), the online calculated desired slip rate λ_d , which is corresponding to the μ_{\max} , can be achieved.

Proof: Applying P_b synthesized in the form of (30) into the proposed system, we have

$$g_1 \frac{de}{dt} = -k_1 e - g_2 \sigma_0 \tilde{z}_0 + g_2 \sigma_1 \frac{\sigma_0 |v_r|}{g(v_r)} \tilde{z}_1 + \Delta + P_{br}, \quad (38)$$

Considering the following p.s.d. candidate Lyapunov function,

$$V_r = \frac{1}{2} g_1 e^2. \quad (39)$$

The derivative of V_r along trajectories in (25), (26) and (38) is

$$\dot{V}_r = -k_1 e^2 + e(-g_2 \sigma_0 \tilde{z}_0 + g_2 \sigma_1 \frac{\sigma_0 |v_r|}{g(v_r)} \tilde{z}_1 + \Delta + P_{br}), \quad (40)$$

Considering (31) proved in Lemma 1 and the structure of V_r , we have

$$\dot{V}_r \leq -k_1 e^2 + \varepsilon \leq -\frac{2k_1}{g_1} V_r + \varepsilon. \quad (40)$$

Utilizing comparison lemma, we have the condition in (37). Thus, $V_r(t)$ exponentially decays and is ultimately bounded. With the help of Assumption 2, the relative velocity v_r tracking error is bounded. Account for the P1, the internal friction states has the properties of boundedness. Through the projection mapping in (25) and (26), the estimates of state \square_0 and \square_1 are bounded by μ_s/σ_0 . Thus the braking pressure input P_b is bounded.

Define the same p.s.d. candidate Lyapunov function V_n as in (21). By substituting (22) and (23), the derivative of V_n along trajectories in (25), (26) and (38) is

$$\begin{aligned} \dot{V}_n &= -k_1 e^2 + e P_{br} - g_2 \sigma_0 \tilde{z}_0 \left(e + \frac{\dot{\hat{z}}_0}{\gamma_0} \right) + \\ &g_2 \sigma_1 \tilde{z}_1 \left(\frac{\sigma_0 |v_r|}{g(v_r)} e - \frac{\dot{\hat{z}}_1}{\gamma_r} \right) + \frac{g_2 \sigma_0 \tilde{z}_0 \dot{\hat{z}}}{\gamma_0} + \frac{g_2 \sigma_1 \tilde{z}_1 \dot{\hat{z}}}{\gamma_1} \\ &= -k_1 e^2 + e P_{br} - \frac{g_2 \sigma_0 \tilde{z}_0}{\gamma_0} \left\{ \dot{\hat{z}}_0 - \left(v_r - \frac{\sigma_0 |v_r|}{g(v_r)} \dot{\hat{z}}_0 - \gamma_0 e \right) \right\} \\ &- \frac{g_2 \sigma_1 \tilde{z}_1}{\gamma_1} \left\{ \dot{\hat{z}}_1 - \left(v_r - \frac{\sigma_0 |v_r|}{g(v_r)} \dot{\hat{z}}_1 + \gamma_1 \frac{\sigma_0 |v_r|}{g(v_r)} e \right) \right\} + \\ &\frac{g_2 \sigma_0 \tilde{z}_0}{\gamma_0} \left(\dot{\hat{z}} - v_r + \frac{\sigma_0 |v_r|}{g(v_r)} \dot{\hat{z}}_0 \right) + \frac{g_2 \sigma_1 \tilde{z}_1}{\gamma_1} \left(\dot{\hat{z}} - v_r + \frac{\sigma_0 |v_r|}{g(v_r)} \dot{\hat{z}}_1 \right) \end{aligned} \quad (41)$$

Substituting the definition of \dot{z} in (8), (28) and (29) in P2 and (32) in Lemma 1, combining the positive parameters in V_n , we have

$$\dot{V}_n = -k_1 e^2 - \frac{g_2}{\gamma_0} \frac{\sigma_0^2 |v_r|}{g(v_r)} \tilde{z}_0^2 - \frac{g_2}{\gamma_1} \frac{\sigma_0^2 |v_r|}{g(v_r)} \tilde{z}_1^2 \leq -k_1 e^2. \quad (42)$$

According to (42), we have $e \in L_2$. Combining the fact that $e \in L_\infty$ and $\dot{e} \in L_\infty$ and utilizing the Barbalat's lemma, we conclude that, $e \rightarrow 0$, as $t \rightarrow \infty$. Thus, by the definition of e and λ in (7), we have $\lambda \rightarrow \lambda_d$, as $t \rightarrow \infty$, which means the μ_{\max} is achieved correspondingly.

IV. SIMULATION RESULTS

Simulations have been performed based on the aircraft system described by aircraft braking system in (8), (9) and aircraft tire/road friction force in (11), (12). The friction parameters and system parameters are given in TABLE I,

TABLE I. SIMULATION PARAMETERS

Name	Value	Units	Name	Value	Units
σ_0	1	1/m	r	0.323	m
σ_1	0.1487	s/m	m	3720	kg
σ_2	0.0038	s/m	J	2.603	kg m ²
μ_C	0.5	-	g	9.8	m/s ²
μ_S	0.9	-	v	50.94	m/s
v_s	12.5	m/s	z_r	1.8	N/m

The initial aircraft speed and wheel linear speed are the same (50.94 m/s). Since the 0s, a braking pressure is applied by the braking actuator on friction parts. The desired slip rate is calculated online, and correspondingly the relative velocity is given to the robust controller as the tracking signal. Noting that, a band-limited white noise signal with power of 0.0001 is injected into the desired slip rate signal from 0s to 7s to simulate external disturbance. The initial values of all integrators are 0. The simulation results show that, the performances of two observers are effective and the system response (slip rate etc.) converge to the real/desired values fast and then recover to their normal values after disturbance.

Figure 3 shows the real value captured from object model and the estimation values of the dual-observer and estimation errors are shown in figure 4. Figure 5 shows the braking pressure order sent to the braking actuator. Figure 6 shows the slip rate calculated by the aircraft and wheel velocity (shown in figure 7) and the desired value calculated online with external disturbance. Once the target of tracking the online calculated desired slip rate is achieved, the maximum adhesion force and deceleration are achieved as well. So we can conclude that, according to the result in figure 6, the desired brake performance is achieved by applying brake pressure signal in figure 5.

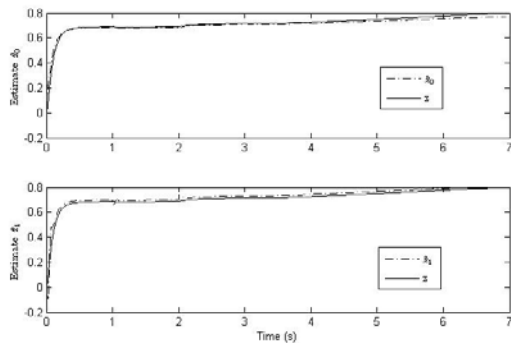


Figure 3 Estimated and real internal friction state values.

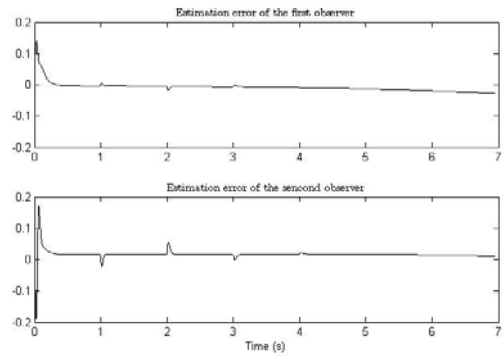


Figure 4 Estimation errors of dual-observer

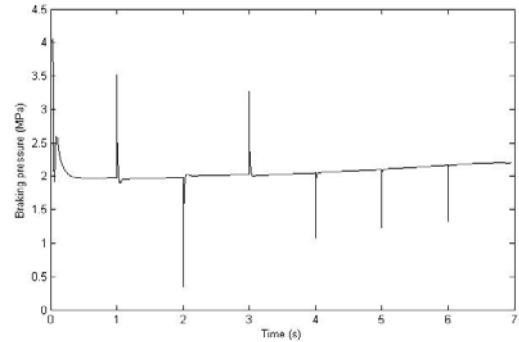


Figure 5 Braking pressure signal applied to the actuator.

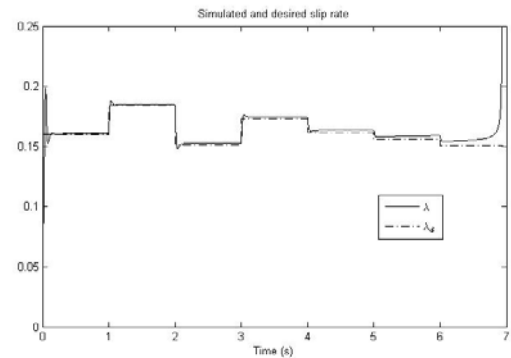


Figure 6 Aircraft system simulated and desired slip rate values.

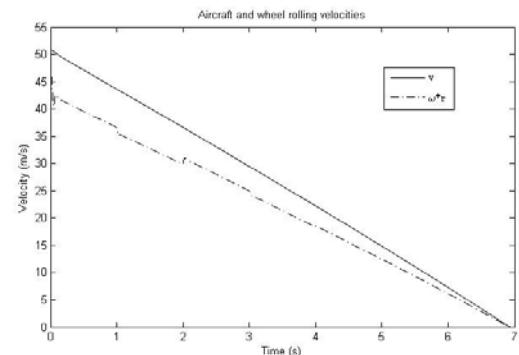


Figure 7 Aircraft and linear wheel velocities.

V. CONCLUSION

In this study, a nonlinear robust controller is proposed based on the LuGre dynamic friction force model. The braking pressure controller is determined by the estimates of unmeasurable internal friction states. A dual-observer is employed to estimate unmeasurable states with the projection mapping and a series of boundedness assumptions in order not to obtain unstable estimates. The simulation results show that the aircraft can be stopped effectively with a near maximum slip rate or deceleration by applying the proposed controller. The asymptotic convergence of the estimated states is also proved theoretically and by simulation results.

REFERENCES

- [1] Wang Ji sen. Nonlinear control theory and application to aircraft antiskid system. Xi'an: Northwestern Poly technical University, 2001(in Chinese).
- [2] Tang Chuanye. Simulation studies on aircraft anti-skid braking system. Xi'an: Northwestern Poly technical University, 2007(in Chinese).
- [3] Li Yuren, Ma Ruiqing, Xue Jing, Xie Lili. Improving variable structure control of aircraft. Journal of Northwestern Poly technical University, 2008,26(6):752-754(in Chinese).
- [4] Tian Guanlai, Xie Lili, Yue Kaixian, Chang Shunkong. Study on optimal control method of an aircraft anti-skid braking system based on slip-ratio. Acta Aeronautica et Astronautica Sinica, 2005, 26(4):461-464(in Chinese).
- [5] Bakker, E., Nyborg, L. and Pacejka, H.B., Tyre modelling for use in vehicle dynamic studies. SAE Paper. No. 870421, 1987.
- [6] C. Canudas de Wit, M. L. Petersen, A. Shiriaev. A new observer for tire/road distributed contact friction. Conference on Decision and Control, Hawaii, USA, 2003.
- [7] J. Yi, L. Alvarez, X. Claeys, R. Horwitz. Adaptive emergency braking control in automated highway system using a dynamic tire/road friction model. Proceedings of 39th IEEE Conference of Decision Control, Sydney, Australia, 2000, pp.456-461
- [8] Yaolong Tan, Ioannis Kanellakopoulos. Adaptive nonlinear friction compensation with parametric uncertainties. Proceeding of the American Control Conference. San Diego: 1999,pp.2511-2513.
- [9] P. Tomei, Robust adaptive friction compensation for tracking control of robot manipulators, IEEE Tran. on Auto. Cont., 45, pp 2164 – 2169, 2000.
- [10] B. Yao, M. Tomizuka, Adaptive robust control of SISO non-linear systems in a semi-strict feedback form, Automatica, 33, pp. 893 – 900, 1997.
- [11] Sastry S, Bodson M. Adaptive control: stability, convergence and robustness. Englewood Cliffs, NJ 07632, USA: Prentice Hall, Inc, 1989.